Proceedings of the 37th International Conference on Ocean, Offshore and Arctic Engineering
OMAE2018
June 17-22, 2018, Madrid, Spain

OMAE2018-78728

NUMERICAL INVESTIGATION OF THE COLLISION DAMAGE AND RESIDUAL STRENGTH OF A FLOATING BRIDGE GIRDER

Yanyan Sha
Center for Autonomous Marine Operations and Systems (AMOS)
Department of Marine Technology
Norwegian University of Science and Technology
Trondheim, Norway
Email: Yanyan.sha@ntnu.no

Jørgen Amdahl
Center for Autonomous Marine Operations and Systems (AMOS)
Department of Marine Technology
Norwegian University of Science and Technology
Trondheim, Norway

Cato Dørum
Norwegian Public Roads Administration,
Hamar, Norway

Zhaolong Yu
Center for Autonomous Marine Operations and Systems (AMOS)
Department of Marine Technology
Norwegian University of Science and Technology
Trondheim, Norway

ABSTRACT

For bridges across wide and deep waterways, fixed foundation structures are not possible to be built due to technical restrictions. Alternatively, pontoon supported floating bridges which do not require fixed foundations can be installed. As the girders of floating bridges may have a low clearance from the sea level, a critical design consideration is the capability of the girder to resist the collision of passing ships. It is hence important to investigate the collision response of the bridge girder and evaluate girder residual strength after the collision. In this paper, finite element (FE) models of a ship deckhouse and a floating bridge girder are established. The girder response to ship deckhouse collision is investigated through integrated numerical simulations. Parametric studies are conducted to compare the girder response for various girder designs and collision scenarios. The residual strength of the girder after in damaged condition is also investigated. Based on the numerical results, a residual strength index (RSI) is proposed for fast prediction of the girder damage level based on the absorbed energy.

INTRODUCTION

Bridge structures are under the threat of accidental ship collisions. Potentially, ship with large kinetic energy may cause serious damages to the bridge structures should a collision accident occur. Therefore, bridges should be designed with an adequate capacity to resist the collision loads without excessive structural damages.

Ship-ship collisions were first studied by Minorsky [1], and Meir-Donberg [2] through collision experiments. Empirical force-deformation relationships and energy absorption curves were obtained. Later, the AASHTO [3] code suggested an equivalent static load for estimating the ship-bridge collision loads. However, Consolazio et al. [4] found the AASHTO-specified loads were substantially larger than those computed via experimentally-validated dynamic analysis for moderate to high energy impacts. More recently, finite element methods have been widely utilized in analyzing vessel-bridge collisions. Yuan and Harik [5] and Consolazio and Cowan [6] calculated the impact force of barge collision with rigid bridge piers. Sha and Hao [7, 8] further studied vessel-pier collisions with an emphasis on structural damages. Base on the numerical results, they proposed simplified equations for a fast estimation of the collision force [9]. Nevertheless, the vessel model in these analyses were typically barges, which have lower and shorter bows than seagoing ships. In addition, the displacement and travel speed of barges, and hence the kinetic energy, are much smaller than merchant ships.

It is worth mentioning that all these works deal with the response of bridge substructures, i.e. piers, piles and pile caps. There has been little focus on the analysis of bridge superstructures against ship collisions [10]. Due to the

increasing height of modern ships, the possibility of ship deckhouse collision with bridge girders has increased significantly. Such accidents can be catastrophic for the road users on the bridge. Since bridge girders are mainly designed for permanent loads and live loads in the vertical direction, they are genuinely weaker in the transverse direction. Therefore, it is crucial to evaluate the girder response under ship deckhouse collisions and strengthen the girders if necessary.

Apart from investigating the structural response during a collision, it is also important to evaluate the residual strength of the bridge after a collision. Floating bridges are exposed to wind and wave loadings during their service life [11]. These environmental loads lead to reaction forces and moments in the bridge structure. To ensure the bridge can survive extreme environmental loadings after a ship collision accident, the residual strength of the bridge girder should be accurately estimated. Many studies have been reported for the residual strength analysis of ship structures [12, 13]. However, the available literature on the residual strength of bridge girders after ship collisions is scarce.

In this work, finite element models of a ship deckhouse and a bridge girder are established based on technical drawings. Numerical simulations of collision between the ship deckhouse and the bridge girder are conducted. Parametric studies are conducted to investigate the collision response of the bridge girder with different steel grade and plate thickness. The effect of vertical impact location is also studied. Finally, the girder residual strength after deckhouse collisions is calculated and a residual strength index (RSI) is proposed for a fast prediction of the girder damage. In this investigation, the local damage and residual strength of the girder in the collision area are focused. The energy levels discussed are only related to local damage. In addition, parts of the collision energy will be transferred into kinetic energy of the bridge. This could be estimated in a global analysis using force-deformation curves form the local analysis as described by Sha and Amdahl [10]. This global analysis is not pursued here.

NUMERICAL MODELLING

FE models of the bridge girder and the ship

A side-anchored floating bridge concept is proposed for Bjørnefjorden strait as shown in Figure 1. The floating bridge contains two cable-stayed spans and thirty-four continuous spans. In the southern part, two main spans are connected to a fixed reinforced concrete tower with stay cables. The remaining continuous spans are supported by floating pontoons. The distance between every two pontoons is 125 m in the continuous part. The total length of the bridge is 5118.5 m. In the current design, the bridge girder in the continuous spans has a relatively low clearance. The height from sea level to the girder bottom is 12 m. This height is lower than the height of deckhouse of the passing ships. It is hence possible that a collision may occur between a ship deckhouse and the bridge girder.

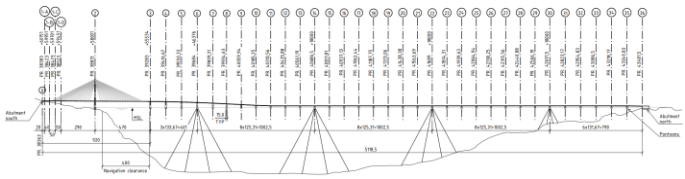

Figure 1. Proposed side-anchored bridge concept.

The girder cross-section in the continuous spans is shown in Figure 2 (a). The thickness of the top plate is 14 mm while the other plates are 12 mm thick. In the longitudinal direction, the shell plating is strengthened by 8 mm and 10 mm thick hat stiffeners. In the transverse direction, 12 mm thick diaphragms with a flange of 250×12 mm are installed every 4 meters. Vertically, 6.3 mm thick hollow circular trusses with a diameter of 219 mm are connected to diaphragms through welding plates. The trusses are connected to the shell model in several points; so as to avoid local overloading of the shell. A detailed analysis of the force transfer in the connection is not included in the present work. Bridge girder plates, longitudinal cap stiffeners and transverse diaphragms were modelled with shell elements while internal trusses were modelled with beam elements as shown in Figure 2 (b). Nine sections, i.e. 36 meters, of the bridge girder were established.

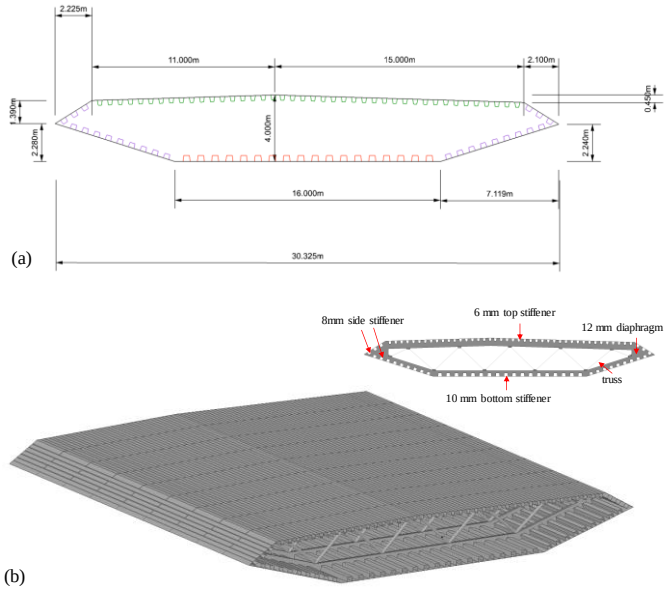

Figure 2. Bridge girder, a) cross section dimensions, b) finite element model.

A finite element model of a container ship with deckhouse was also developed as shown in Figure 3. The overall ship was modelled coarsely while the deckhouse was modelled in detail as this part will get in direct contact with the bridge girder. The plates, decks, girders and stiffeners in the ship deckhouse were modelled with shell elements. The thickness of these structural members varies from 8 mm to 18 mm. The width, height and depth of the deckhouse are 15 m, 15.5 m and 17.6 m, respectively.

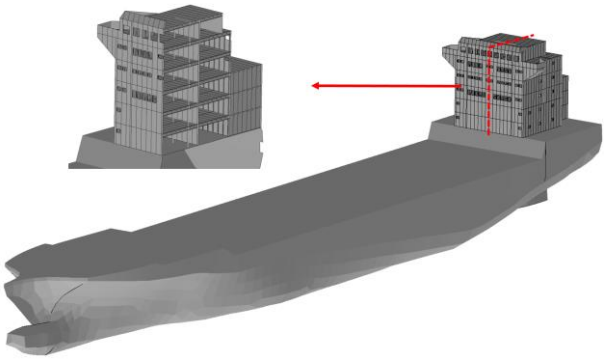

Figure 3. Ship-girder collision accidents.

For the shell elements in the bridge girder and the ship deckhouse, the mesh size should be maintained within 5-10 times the plate thickness to obtain sufficiently accurate predictions of the strain and fracture. As the structural members have a thickness ranges from 8-18 mm, a minimum mesh size of 80 mm was used in the bridge girder and in the ship deckhouse. For the other parts of the ship, a larger mesh was used as they are not expected to endure significant structural deformations. An illustration of the mesh is shown in Figure 4.

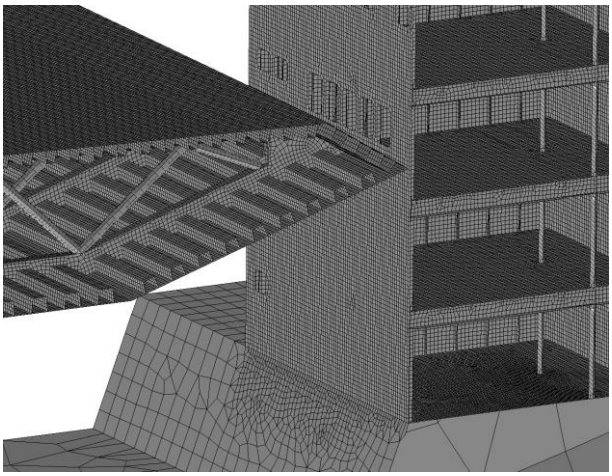

Figure 4. Mesh illustration of the ship and the girder.

Material modelling

A material model developed by Alsos et al. [14] was used in this study for the steels in the ship. The material was assumed to have isotropic plastic property and modelled using plane stress J2 flow theory. The equivalent stress-strain curve is represented by a modified power law formulation including the plateau strain,

$$\sigma_{\text{eq}} = \begin{cases} \sigma_{\text{y}} & \text{if } \varepsilon_{\text{eq}} < \varepsilon_{\text{plat}} \\ K\left(\varepsilon_{\text{eq}} + \varepsilon_0\right)^n & \text{otherwise} \end{cases}, \tag{1}$$

where K and n are material parameters. ε_{eq} is the equivalent plastic strain at the plateau exit and σ_{y} denotes the initial yield stress. The strain ε_0 allows the plateau and the power-law expression to intersect at ($\varepsilon_{\text{plat}}$, σ_{y}) and is obtained by,

$$\varepsilon_0 = \left(\frac{\sigma_{\text{y}}}{\text{K}}\right)^{\frac{1}{\text{n}}} - \varepsilon_{\text{plat}} . \tag{2}$$

The material failure was considered by incorporating the Rice-Tracey-Cockcroft-Latham (RTCL) damage criterion [14]. The element size for the FE model is around 5 to 10 times of the plate thickness. To get a better prediction of strain and fracture, the damage criterion is scaled according to mesh size based on the following equation,

$$\varepsilon_{\text{cr}} = n + \left(\varepsilon_{\text{n}} - n\right)\frac{t}{l_{\text{e}}}, \tag{3}$$

where ε_{cr} is the critical strain and ε_{n} is the failure strain in uniaxial tension for mesh size l_{e} and plate thickness t .

The container ship is fabricated in mild steel while the bridge girder is constructed of high-strength steel. The characteristic yield stresses for the deckhouse and the girder were 275 MPa and 420 MPa respectively. Detailed parameters for the two materials are tabulated in Table 1 and the true stress-strain curves are plotted in Figure 5.

Table 1. Material properties of the deckhouse and the girder.

Items	Deckhouse	Girder
Density	7850 kg/m^3	7850 kg/m3
Young's modulus	206 GPa	206 GPa
Poisson's ratio	0.3	0.3
Yield stress	275 MPa	420 MPa
Strength index (K)	740 MPa	863 MPa
Strain index (n)	0.24	0.15

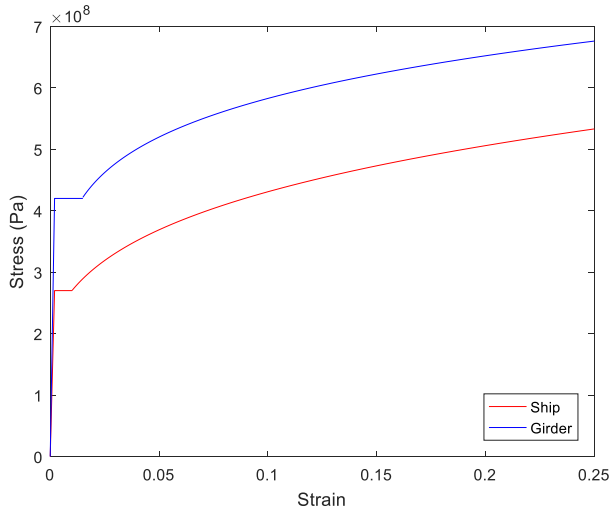

Figure 5. True stress-strain curves of the steel material

NUMERICAL COLLISION SIMULATIONS

Figure 6 shows the setup for the simulation of the local deckhouse-girder collisions. The deckhouse was assumed to

collide with the middle part of the girder. In the simulation, the bridge girder was fixed in all translational and rotational degrees of freedom at both ends. For the local analysis, the ship was assumed to travel with a constant speed of 10 m/s, which is sufficiently large to reduce CPU consumption and low enough to avoid significant inertia effects. Any strain rate hardening was not accounted for.

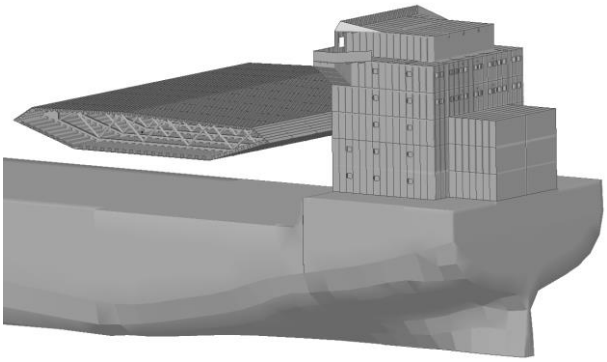

Figure 6. Collision setup.

Collision response

Figure 7 shows the structural damage at a crushing depth of 5 m, 10 m and 15 m, respectively. Initially, the bridge girder cuts into the deckhouse between two horizontal decks. The deckhouse endures excessive damages while the bridge girder is virtually intact. When the crushing depth is 10 m, the girder keeps penetrating into the deckhouse, the horizontal deck in the ship deckhouse interacts with the girder plates. Inward bending of the outer plates and the buckling of the internal trusses can be observed in the girder. When the crushing depth is 15 m, the structural damage in the girder becomes significant. Large deformation of the diaphragm webs and flanges can also be observed as shown in Figure 8.

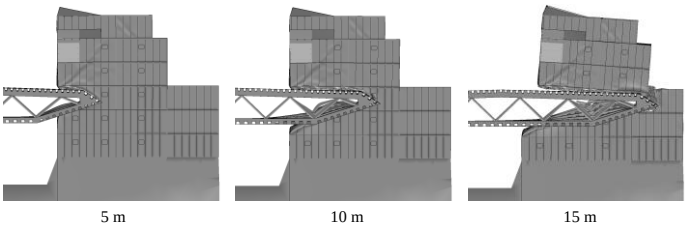

Figure 7. Structural deformations.

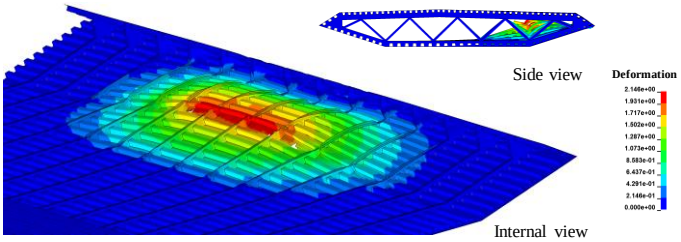

Figure 8. Girder deformation at 15 m crush depth.

The force-deformation curves for both structures are shown in Figure 9. The deckhouse has a crush depth of 17.5 m while the girder undergoes a much smaller deformation of 2.5 m. It means the ship deckhouse endures a much more severe damage than the girder and dissipates most of the collision energy. Three major force peaks develop as the girder edge contacts with the vertical bulkheads in the deckhouse. The force level is approximately 20-25 MN outside these peaks. This force level is quite substantial compared to the force for the standard of the supply vessel bow impacts with offshore structures [15].

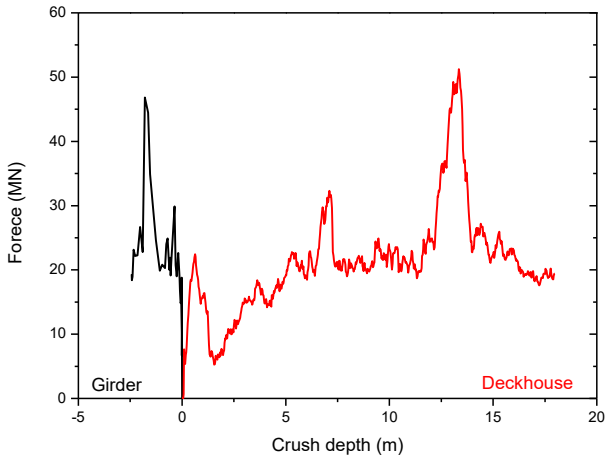

Figure 9. Force-deformation curves.

PARAMETRIC STUDY

To further investigate the effect of various girder configurations and collision scenarios, parametric studies were conducted in this section. The effect of girder steel grade, girder plate thickness and impact height is discussed.

Effect of girder steel grade

A floating bridge girder may require a higher strength to resist the extreme wind and wave loadings. An easy, yet effective method, is to increase the steel grade in the bridge girder. In this section, the collision response is investigated for the girder with a higher steel grade (S460). The same ship deckhouse collision is simulated and the force-displacement curve of the collision is shown in Figure 10. The force-deformation curve of the original girder with a steel grade S420 is plotted in the same figure for comparison purpose.

In both cases, the strength of the bridge girder is much larger than that of the deckhouse. Therefore, the deckhouse strength dominates the damage level and governs the force amplitude. Increasing the steel grade does not have an obvious contribution in improving the collision resistance of the girder in the present case. It should be noted that this suggestion is only intended for the girder design against a deckhouse collision. For bridge girders subjected to ship bow impacts, a higher steel grade may be required due to the relatively higher strength of the ship bow.

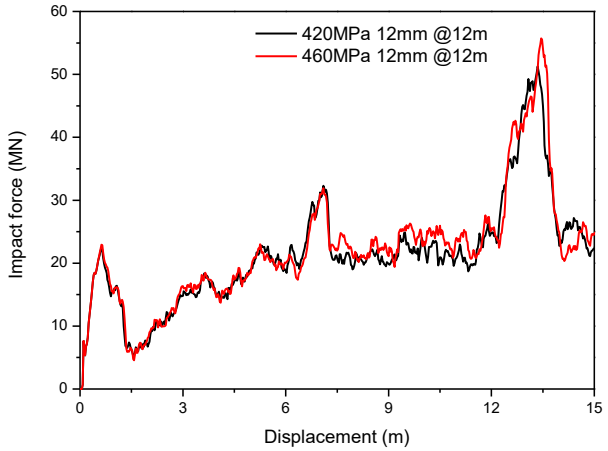

Figure 10. Effect of girder steel grade.

Effect of girder plate thickness

The girder strength can also be varied by changing the thickness of the outer plates. In the initial design, the side and bottom plates are 12 mm thick. To investigate the effect of girder plate thickness on the collision response, a thinner thickness of 10 mm and a thicker thickness of 14 mm are modelled and simulated for comparison.

Figure 11 shows the force-displacement curves of the deckhouse-girder collision for different girder plate thickness. The force level of the first peak at about 1 m displacement increases with an increasing plate thickness. This is because the girder with 10 mm thick plates has a lower strength than the two other girders. The girder edge deforms when it contacts with the deckhouse and releases the impact force. The girder with 14 mm thick plates undergoes less local deformation and it mobilizes the deckhouse structures of the adjacent deck below. Consequently, the resistance of the deckhouse is larger until fracture occurs. Since the overall girder strength is larger than the deckhouse for all three case, the girder is able to overcome the first peak and the rest of the curve is quite similar for all cases.

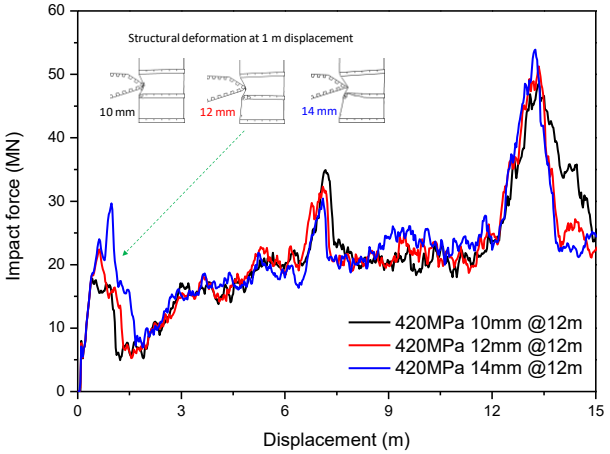

Figure 11. Effect of girder plate thickness.

Effect of the vertical impact location

The floating bridge and the ship are both floating structures which may move vertically due to the sea waves. Thus, the relative vertical impact location can vary due to their heave motions. To evaluate the effect of the vertical impact location, collision analyses of two higher impact heights of 13.5 m and 15 m as shown in Figure 12 are simulated.

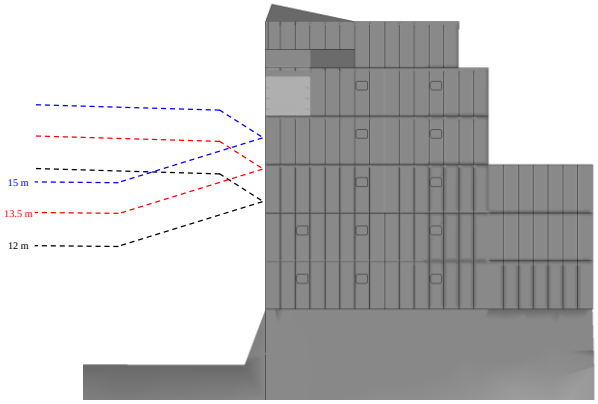

Figure 12. Illustration of the three impact locations.

Figure 13 compares the force-displacement curves for the three impact heights. The first peaks of an impact height of 12 m and 15 m are comparable as they are both dominated by the membrane of the front plate. For an impact height of 13.5 m, a delayed higher first peak can be observed. This is because the crushing of the horizontal deck in the ship deckhouse also contributes to the resistance in this early stage. Later, the force levels are generally in the same range until 12 m displacement. For the lowest impact height of 12 m, the collision force attains a large local peak of 51 MN as the girder interacts with the rear bulkhead of the deckhouse. The peak, however, does not exist in force-displacement curves of the other two cases with higher impact locations. This is because the girder tends to exert an overturning moment to the upper part of the deckhouse instead of crushing against the rear bulkhead. In these two cases, sliding interaction dominates the impact force, which results in relatively 'smooth' force-displacement curves. The structural deformations at 15 m ship displacement for the three impact locations are included in Figure 13.

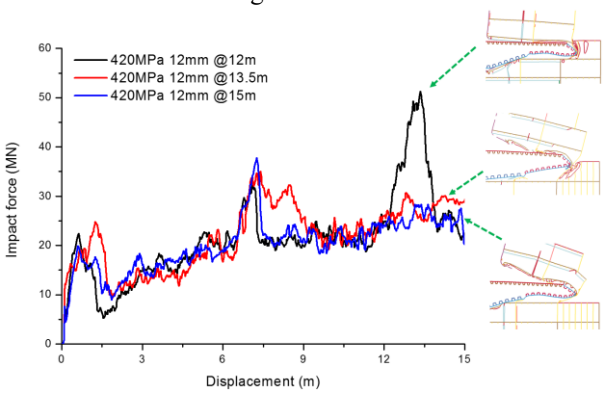

Figure 13. Effect of the vertical impact location.

GIRDER RESIDUAL STRENGTH

It is important to ensure that the bridge girder can survive the extreme wave loadings after a ship collision accident. The wave loads will strongly influence the heave motion of the pontoons, which leads to the change of the weak axis bending moment, torsional moment and vertical shear force in the bridge girder. This section describes a residual strength analysis of the local girder model shown in Figure 2. The global bridge response for the environmental loadings is not discussed.

Analysis setup

The residual strength analysis is carried out in three steps. 1). The ultimate strength of the bridge girder in an intact condition is first obtained as the reference ultimate strength. 2). A deckhouse-girder collision as shown in the previous section is simulated to introduce the structural deformation and damage in the bridge girder. The stress state and the deformation of the damaged girder are saved for the subsequent estimation of residual strength. 3). With the damaged condition obtained from Step 2, the residual strength of the girder is calculated following the same approach as in Step 1.

In the simulation, a proper boundary condition should be defined first. As shown in Figure 14, two reference nodes at the neutral axis of the girder cross-section are defined at the fore and aft section of the girder. All translational and rotational degrees of freedom of the end nodes are coupled to the reference nodes through rigid links. To obtain the ultimate and strength of the bridge girder, a gradually increased external rotation is applied to the two reference points until the girder fails. In this study, only the bending moment about the bridge weak axis is analyzed. The bridge capacity for other forces and moments can be evaluated in the same manner. In addition to the residual strength assessment, the girder response subjected to cyclic wave loadings in the damaged state is also discussed.

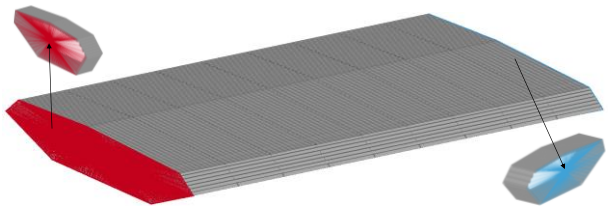

Figure 14. Reference nodes and boundary conditions

Ultimate strength

In LS-DYNA, both the implicit and explicit solvers can be used for ultimate strength analyses. Using the explicit solver is relatively easy as no convergence check is required during the simulation. However, the external moment should be applied in a slow manner to avoid the dynamic effect. The advantage of the implicit analysis is that this can be done statically, thus eliminating dynamic effects. However, it can be difficult to reach convergence for structures with excessive damages.

In this study, the explicit solver is selected to analyze the ultimate and the residual strength of the bridge girder. As discussed above, the external rotation should be applied at a slow speed that does not induce substantial dynamic effects. After a number of trial-and-error simulations, a loading speed of 0.016 rad/s is used. To further verify the accuracy of the explicit analysis, an implicit analysis is conducted to compare with the results obtained from the explicit analysis.

An external rotation about the bridge weak axis is applied to the reference nodes of the girder section in the intact state. The weak axis bending moments of the girder obtained from the two methods are shown in Figure 15. It is observed that the ultimate strengths predicted by the two methods are almost identical. In addition, the first yield of the weak axis bending moment is around 750 MN m, which is similar to the first yield value, estimated by the linear theory. This suggests that the explicit analysis approach is able to accurately predict the ultimate strength of the girder. The ultimate strength of the intact state is then used as the benchmark strength for the girder.

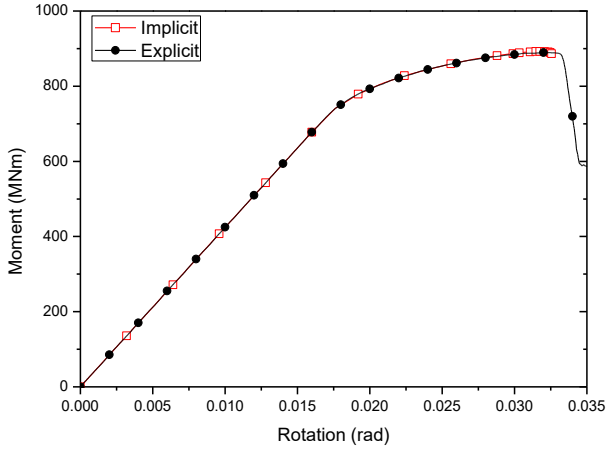

Figure 15. The explicit analysis versus the implicit analysis.

Collision damage

To evaluate the residual strength of the bridge girder after a deckhouse collision, the damaged girder condition should first be defined. The collision simulation has been discussed in detail in the previous section. During the collision, four girder damage levels are selected as shown in Figure 16. The stress contour and girder deformation are shown in the figure. The corresponding residual strength will be calculated and compared with the ultimate strength in the intact condition. Table 2 lists the energies absorbed by the girder and the deckhouse in the simulated cases.

Table 2. Energies dissipations (in MJ).

	D0	D1	D2	D3	D4
Girder	0	28	46	107	193
Deckhouse	0	65	136	259	340
Total	0	93	182	366	533

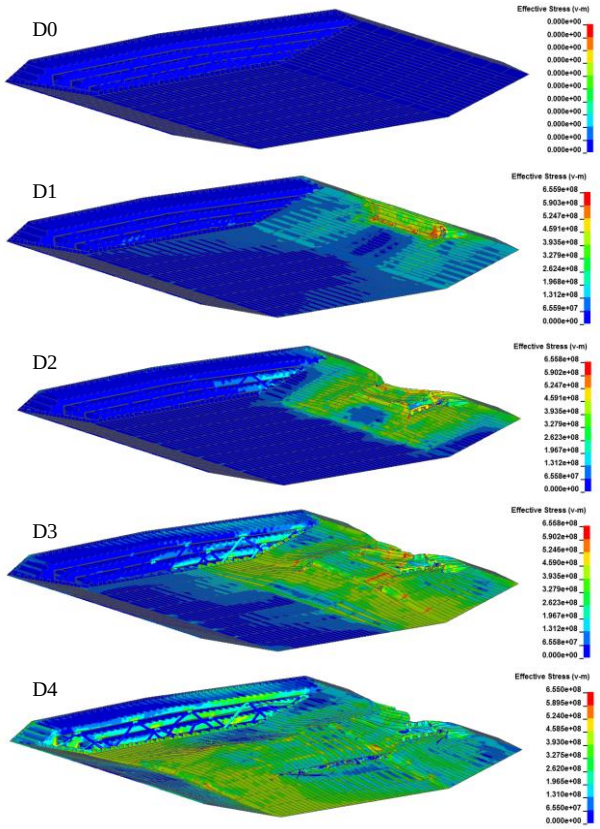

Figure 16. Girder stress states of various damage levels.

Residual ultimate strength

After the collision, both the deformed geometry and stress state of the girder after the collision should be used as the initial condition of the residual strength analysis. The new girder geometry is obtained by updating the coordinates of the nodes in the deformed zone while the residual stress caused by the collision is used as the initial stress in the girder. Then, the same loading condition as in the ultimate strength analysis is applied to the girder to calculate the residual strength.

The weak axis bending moments of the four damage conditions are shown in Figure 17. For comparison purpose, the ultimate strength of the girder in the intact condition is also plotted in the figure. It can be observed that for case D1 and D2, the reduction of the ultimate strength is insignificant. For these small damages, the girder maintains virtually its capacity. However, when the damage in the girder is larger (case D3), a clear reduction in the ultimate strength can be observed. A dramatic drop in the girder strength can be found when the girder absorbs a collision energy of 193 MJ (case D4).

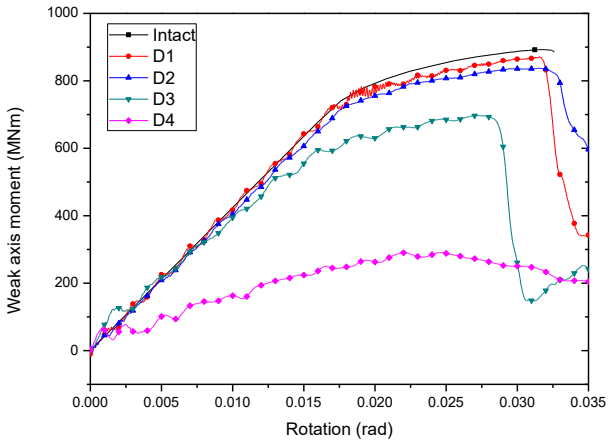

Figure 17. Weak axis bending moments in the intact and the damaged states.

Residual strength index

For a fast estimation of the girder damage level after a ship deckhouse collision, a residual strength index (RSI) is proposed. It is defined as the ratio of the ultimate strength in damage state versus that in the intact state. The RSI can be obtained by:

$$RSI = \frac{M_d}{M_i}, \tag{4}$$

where M_d is the ultimate moment capacity in the damaged state and M_i is the ultimate moment capacity in the intact state.

For the four damage levels as discussed above, the RSI is obtained from the results shown in Figure 17. The RSI and the corresponding girder energy are listed in Table 3.

Table 3. RSI for different energy levels.

Case	D1	D2	D3	D4
Girder internal energy (MJ)	28	46	107	193
RSI	0.98	0.94	0.78	0.33

The girder energy dissipation versus RSI curve is shown in Figure 18. With this curve, the girder damage level after a deckhouse collision can be quickly estimated based on the collision energy. For collision scenarios where the local energy dissipation in the girder is less than 200 MJ, the girder damage can be easily obtained by intersecting the corresponding RSI with the curve. It should be noted that the curve is based on the deckhouse from a container ship as shown in Figure 3, the damage pattern of the girder can vary if collided by a different deckhouse. Nevertheless, the same procedure can be applied for generating the RSI and the corresponding energy curves.

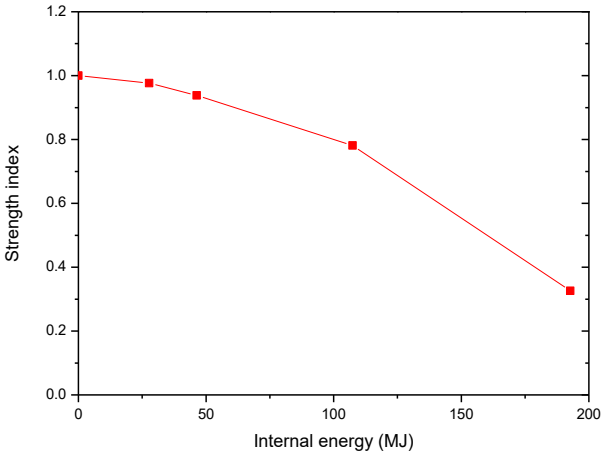

Figure 18. Girder internal energy versus RSI.

CONCLUSIONS

In this study, finite models of a container ship deckhouse and a bridge girder section were developed. Integrated numerical simulations were conducted to investigate the local response of the girder and deckhouse in a collision. It is found the bridge girder which has a higher strength only endures minor deformation while the relatively weaker deckhouse suffers excessive damage. The impact force for the deckhouse-girder collision is approximately 20-25 MN except for the peaks due to the main vertical plates in the deckhouse.

A Parametric study shows that increasing the steel grade of the bridge girder has a minor influence on the impact force. The thickness of the girder plate will influence the amplitude of the first peak of the impact force. However, it does not change the overall collision response, since the force level is governed by the penetration resistance of the deckhouse. Changes in the vertical impact location will result in different failure modes of the deckhouse and thus the impact response is different.

A residual strength index for the collision scenario studied is presented for fast estimation of the girder residual strength based on the absorbed energy. When the total energy dissipation in the deckhouse and the girder is less than 46 MJ, the reduction of the ultimate strength is very small (6%). However, the girder residual strength drops to only 33% when the energy attains 193 MJ. For both cases, the ship collision energy will be larger as some of the kinetic energy is transferred to the kinetic energy in the bridge.

The static, residual strength of the girder is a first parameter to consider. Cyclic wave loads may lead to incremental collapse or failure due to alternating plasticity. This will be pursued in future studies.

ACKNOWLEDGEMENTS

Dr Martin Storheim is gratefully acknowledged for providing the numerical model of the ship. This work was supported by the Norwegian Public Roads Administration (project number 328002) and in parts by the Research Council of Norway through the Centres of Excellence funding scheme, project AMOS (project number 223254). The support is gratefully acknowledged by the authors.

REFERENCES

[1] V. Minorsky, An analysis of ship collisions with reference to protection of nuclear power plants. 1958, Sharp (George G.) Inc., New York.

[2] K. Meir-Dornberg, Ship collisions, safety zones, and loading assumptions for structures in inland waterways. VDI-Berichte, 1983. 496(1): p. 1-9.

[3] AASHTO, Guide Specification and Commentary for vessel collision design of highway bridges. American Association of State Highway and Transportation Officials, Washington, DC, 1991.

[4] G.R. Consolazio, et al., Barge impact testing of the St. George Island causeway bridge. 2006: Department of Civil and Coastal Engineering, University of Florida.

[5] P. Yuan and I.E. Harik, Equivalent barge and flotilla impact forces on bridge piers. Journal of Bridge Engineering, 2009. 15(5): p. 523-532.

[6] G.R. Consolazio and D.R. Cowan, Nonlinear analysis of barge crush behavior and its relationship to impact resistant bridge design. Computers & structures, 2003. 81(8): p. 547-557.

[7] Y. Sha and H. Hao, Nonlinear finite element analysis of barge collision with a single bridge pier. Engineering Structures, 2012. 41: p. 63-76.

[8] Y. Sha and H. Hao, Laboratory tests and numerical simulations of CFRP strengthened RC pier subjected to barge impact load. International Journal of Structural Stability and Dynamics, 2015. 15(02): p. 1450037.

[9] Y. Sha and H. Hao, A simplified approach for predicting bridge pier responses subjected to barge impact loading. Advances in Structural Engineering, 2014. 17(1): p. 11-23.

[10] Y. Sha and J. Amdahl, Local and global responses of a floating bridge under ship-girder collisions. Journal of Offshore Mechanics and Arctic Engineering, 2018. (under review).

[11] Y. Sha, et al., Numerical investigations of the dynamic response of a floating bridge under environmental loadings. Ships and Offshore Structures, 2018.

[12] J. Gordo and C.G. Soares, Tests on ultimate strength of hull box girders made of high tensile steel. Marine Structures, 2009. 22(4): p. 770-790.

[13] J. Parunov, S. Rudan, and B.B. Primorac, Residual ultimate strength assessment of double hull oil tanker after collision. Engineering structures, 2017. 148: p. 704-717.

[14] H.S. Alsos, J. Amdahl, and O.S. Hopperstad, On the resistance to penetration of stiffened plates, Part II: Numerical analysis. International Journal of Impact Engineering, 2009. 36(7): p. 875-887.

[15] N. Norsok, 004, Design of steel structures. Standards Norway, Rev, 2004. 2.